Zeolite Catalysis

DOI: 10.1002/anie.201407030

Isolation of the Copper Redox Steps in the Standard Selective Catalytic Reduction on Cu-SSZ-13**

Christopher Paolucci, Anuj A. Verma, Shane A. Bates, Vincent F. Kispersky, Jeffrey T. Miller, Rajamani Gounder, W. Nicholas Delgass, Fabio H. Ribeiro, and William F. Schneider**

Abstract: *Operando X-ray absorption experiments and density functional theory (DFT) calculations are reported that elucidate the role of copper redox chemistry in the selective catalytic reduction (SCR) of NO over Cu-exchanged SSZ-13. Catalysts prepared to contain only isolated, exchanged Cu^{II} ions evidence both Cu^{II} and Cu^{I} ions under standard SCR conditions at 473 K. Reactant cutoff experiments show that NO and NH_3 together are necessary for Cu^{II} reduction to Cu^{I}. DFT calculations show that NO-assisted NH_3 dissociation is both energetically favorable and accounts for the observed Cu^{II} reduction. The calculations predict in situ generation of Brønsted sites proximal to Cu^{I} upon reduction, which we quantify in separate titration experiments. Both NO and O_2 are necessary for oxidation of Cu^{I} to Cu^{II}, which DFT suggests to occur by a NO_2 intermediate. Reaction of Cu-bound NO_2 with proximal NH_4^+ completes the catalytic cycle. N_2 is produced in both reduction and oxidation half-cycles.*

NO_x selective catalytic reduction (SCR) to N_2 with NH_3 is commonly used to control emissions from combustion sources. Standard SCR is a redox reaction between NO and NH_3 [Eq. (1)]

$$4\,NH_3 + 4\,NO + O_2 \rightarrow 4\,N_2 + 6\,H_2O \quad (1)$$

and under useful conditions is selective for NH_3 oxidation by NO over oxidation by the O_2 that is typically present in great excess.[1] Mobile applications demand greater hydrothermal stability than offered by the vanadia catalysts used in stationary applications. Only with the discovery of hydrothermally stable Fe- and Cu-exchanged chabazite (CHA) catalysts, including Cu-SSZ-13 (aluminosilicate) and Cu-SAPO-34 (silicoalumino-phosphate),[2] has NO_x SCR become commercially viable for mobile source emissions control.

The CHA framework contains interconnected 4-, 6-, and 8-membered rings (4-MR, 6-MR, 8-MR). Substitution of Al for Si in SSZ-13 and of Si for P in SAPO-34 introduces anionic coordination sites for exchanged Cu^{I} and/or Cu^{II} ions, H^+, NH_4^+, and other cations. The identities and numbers of exchanged cationic species depend on the framework Si:Al ratio, the distribution of Al atoms in the framework, the total Cu content and Cu exchange method, and the treatment history of the material. Furthermore, the Cu coordination environment[3] and oxidation state can change under reaction conditions.[4]

The preferred Cu exchange sites at low Cu loading in SSZ-13 are well established. DFT calculations identify a 6-MR containing two framework Al atoms as the most stable exchange site for a Cu^{II} ion in SSZ-13.[3,5] Temperature-programmed reduction experiments[6] and electron paramagnetic resonance spectroscopy[7] both show that these exchange sites are populated first at low Cu:total Al (Cu:Al) ratios. The number of such exchange sites depends only on the Si:Al ratio if Al atoms are distributed randomly within the SSZ-13 framework. Numerical simulations show that a Cu:Al ratio of 0.2 is sufficient to fill all candidate 6-MR sites with Cu^{II} at a Si:Al ratio of 4.5.[5a] UV/Vis/near-IR spectroscopy,[5a] X-ray absorption spectroscopy (XAS),[8] and NH_3 titration of residual Brønsted acid sites[9] together show that SSZ-13 samples prepared with a Si:total Al ratio of 4.5 and loaded with Cu:Al ≤ 0.2 contain exclusively Cu^{II} ions isolated in 6-MR. Furthermore, Cu-SSZ-13 samples containing only isolated Cu^{II} are active for standard SCR at 473 K,[3,5a,10] with SCR rates that are directly proportional to the number of 6-MR Cu^{II} ions.[3,5a,10]

Although standard SCR rates correlate with initial 6-MR Cu^{II} content, this oxidation state is not maintained during catalysis. In qualitative agreement with the XAS results by

[*] C. Paolucci, Dr. W. F. Schneider
Department of Chemical and Biomolecular Engineering
University of Notre Dame
182 Fitzpatrick Hall, Notre Dame, IN 46556 (USA)
E-mail: wschneider@nd.edu
A. A. Verma, Dr. S. A. Bates, Dr. V. F. Kispersky, Dr. R. Gounder, Dr. W. N. Delgass, Dr. F. H. Ribeiro
School of Chemical Engineering, Purdue University
480 Stadium Mall Drive, West Lafayette, IN 47907 (USA)
E-mail: fabio@purdue.edu
Homepage: https://engineering.purdue.edu/~catalyst/
J. T. Miller
Chemical Sciences and Engineering Division
Argonne National Laboratory
9700 S Cass Avenue, IL 60439 (USA)

[**] Financial support was provided by the U.S. Department of Energy (DoE) vehicle technology program under contract number DE-EE0003977, and by the National Science Foundation GOALI program under award number 1258715-CBET. Support for J.T.M. was provided under the auspices of the U.S. DOE, Office of Basic Energy Sciences, Division of Chemical Sciences, Geosciences, and Biosciences under contract number DE-AC0-06CH11357. We would like to thank Sachem, Inc. for their gracious donation of the structure-directing agent used in the synthesis of SSZ-13. We thank Dr. Paul Dietrich and Atish Parekh for help in conducting X-ray absorption experiments at the APS. We also thank the Center for Research Computing at Notre Dame for support of computational resources.

Supporting information for this article is available on the WWW under http://dx.doi.org/10.1002/anie.201407030.

Doronkin et al.,[11] operando XAS reveals both Cu^{II} and Cu^{I} ions under standard SCR conditions,[4a,11] and their proportions have been quantified under differential conditions in the absence of transport limitations on Cu-SSZ-13 samples that initially contained only 6-MR Cu^{II} ions.[12] DFT calculations show that the oxidation state of 6-MR Cu can be changed by adsorbates and that both Cu^{I} and Cu^{II} forms have comparable thermodynamic stability under SCR conditions.[4a] Kwak et al. proposed that adsorbed NO reduces Cu^{II} to Cu^{I}, based on ambient temperature ex situ vibrational and ^{15}N nuclear magnetic resonance spectroscopies.[13] More recently, Gao et al.[14] proposed that co-adsorption of NO and NH_3, reduces Cu^{II} to Cu^{I} based on ex situ vibrational spectroscopy. Similar reaction mechanisms were proposed for standard SCR on Fe-based zeolites. Klukowski et al.[15] proposed the participation of both NO and NH_3 in the reduction of Fe sites. Taken together, this evidence indicates that Cu and Fe redox chemistry occurs during standard SCR.

In this contribution, we report operando experiments and DFT computations and analysis that isolate and explain the response of a Cu-SSZ-13 catalyst, initially prepared to contain only 6-MR Cu^{II} ions, to standard SCR reaction conditions at 473 K and upon cutoff of each reactant under plug flow conditions. We show that standard SCR is associated with Cu redox chemistry between the Cu^{II} and Cu^{I} states, that the reduction half-cycle requires both NH_3 and NO, that each reduction event generates a Brønsted acid site proximal to Cu^{I} that binds a catalytically relevant NH_4^+ species, and that the oxidation half-cycle requires NO and O_2 and consumes this NH_4^+. We use these results to propose a redox mechanism for standard SCR of NO with NH_3, in which N_2 is formed as a product in both the reduction and oxidation half-cycles.

Two Cu-SSZ-13 catalysts (Cu:Al = 0.11 and 0.16, Si:Al = 4.5) were prepared to contain exclusively isolated Cu^{II} ions.[5a,9] Preparation details are given in Section S1 in the Supporting Information and characterization data are presented elsewhere.[5a,9] These catalysts were placed in glassy carbon tubes in a custom-built reactor developed to collect operando SCR kinetics under plug flow conditions[4a,12] and exposed to standard SCR mixtures at 473 K. Further details are found in Section S2. Under differential conditions (< 20% NO conversion) the observed steady-state SCR rates were 4.8×10^{-3} and 5.1×10^{-3} mol NO (mol Cu s)$^{-1}$ for the Cu:Al 0.11 and 0.16 samples, respectively, each within a factor of 1.3 of rates on the same catalysts measured elsewhere, as detailed in Section S3.[5a] The reproducibility of the rates confirms the operando XAS reactor operates under plug flow, while the constant SCR turnover rate certifies by the Koros–Nowak test that the kinetic data are not corrupted by heat and mass transfer artifacts.[16] The operando X-ray absorption near edge structure (XANES) spectra of Cu were fitted to linear combinations of XANES references including an isolated Cu^{II} ion in SSZ-13, an isolated Cu^{I} ion in SSZ-13, and a hydrated isolated Cu^{II} ion ($[Cu(H_2O)_6]^{II}$), as detailed in Sections S4 and S5. The first column of Figure 1 shows that nearly 30% of Cu is present as Cu^{I} and 70% as Cu^{II} under standard SCR conditions in both samples. Corresponding XANES spectra and quantification results are reported in Section S6 and Table S4.

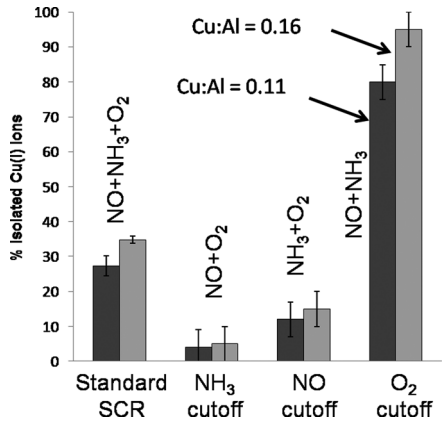

Figure 1. Percentage of isolated Cu^{I} relative to the total number of Cu ions under various steady-state flow conditions. 5% H_2O was present in all the cutoff mixtures. Standard SCR conditions are 320 ppm NO, 320 ppm NH_3, 10% O_2, and 5% H_2O, at 473 K.

Reactant cut-off experiments probe the effect of gas composition on the Cu oxidation states. Starting from steady-state standard SCR conditions, the flow of one reactant was switched to an inert CO_2 tracer to maintain a constant total gas flow rate, as detailed in Section S2. NH_3 cut-off experiments left behind a feed mixture of NO and O_2 and NO cut-off left behind a feed of NH_3 and O_2. In both experiments, feed streams contained 5% H_2O and an appropriate amount of balance He gas. After NH_3 or NO cut-off, NO consumption rates decreased with time to undetectable levels. The steady-state Cu^{I} percentage (Figure 1) decreased to about 5% after NH_3 cutoff and 12% after NO cutoff (XANES before and after cutoffs detailed in Sections S6.1 and S6.2, respectively), indicating that the feed streams lost their reduction ability when either NH_3 or NO was absent at 473 K. Thus, we conclude that NO or NH_3 separately, at concentrations typical of standard SCR, cannot reduce isolated Cu^{II} to Cu^{I} ions.

To explain these results, we used DFT to compute free energies and oxidation states associated with reactant adsorption on a 6-MR Cu^{II} ion. We used an SSZ-13 supercell (Si:Al ratio of 5:1) containing two Al in a 6-MR, and placed a Cu ion in the preferred exchange site.[5a] We probed molecular adsorption of NH_3, H_2O, O_2, N_2, and NO at this Cu site using the hybrid screened exchange (HSE06) exchange-correlation functional, which provides superior estimates of reaction energies involving NO.[17] Initial adsorbate geometries were chosen from low-energy structures visited during preliminary ab initio molecular dynamics (AIMD) simulations and were subsequently optimized; relaxed structures and binding energies are in Sections S10 and S13 and additional computational details in Section S9. NH_3 and H_2O adsorption are most exothermic and diatomic binding to the Cu site is only modestly exothermic.

To relate the HSE06 adsorption energies to free energies at the experimental reaction conditions, ΔG(473 K), we used isothermal AIMD and the PBE functional to construct the potential of mean force (PMF) associated with drawing adsorbed NH_3 from the SSZ-13 central cage to the Cu^{II} site (details in Sections S9.3 and S11). The PBE functional is more cost-effective than HSE06 and provides an NH_3 binding

energy within 8 kJ mol^{-1} of the HSE06 value. The free energy difference at 473 K is −62 kJ mol^{-1} from the integrated PMF. The free energy of confinement of an ideal gas within a zeolite cage has been estimated from adsorption experiments[18] and Grand-Canonical Monte Carlo simulations[19] to be +20–30 kJ mol^{-1}. The upper value of 30 kJ mol^{-1} is appropriate to the small-pore SSZ-13. Combining these, we estimate the net NH_3 adsorption free energy relative to an NH_3 ideal gas is −32 kJ mol^{-1}. This free energy difference is comparable to that computed for an ideal NH_3 gas that retains the equivalent of 2/3 of its free translational entropy upon adsorption, also in agreement with experimental results for O_2 adsorption in chabazite.[20] Consistent with this picture, the NH_3 adsorbate is quite dynamic in the MD simulations even at the equilibrium Cu–NH_3 distance.

Figure 2 A reports 473 K adsorption free energies computed from the HSE06 energies and an assumed loss of 1/3 of the gas-phase translational entropy by each adsorbate. Only NH_3 and H_2O compete for 6-MR Cu sites under standard SCR conditions. The diatomics are unlikely to populate these sites. The binding preference computed for NH_3 over H_2O is consistent with XANES spectra collected after NH_3 cut-off experiments, which show the proportions of hydrated Cu^{II} to increase from 7 ± 3 % to 41 ± 5 % on the 0.11 Cu:Al sample and from 3 ± 3 % to 48 ± 5 % on the 0.16 Cu:Al sample (details are found in Tables S4 and S7).

We determined the Cu oxidation state from both integrated Cu density of states and Bader charges, using the isolated Cu ion in the 6-MR as a Cu^{II} standard. Results from both analyses were consistent across all calculations (details are in Sections S12 and S13). Figure 2 A summarizes the Bader results in the color-coding of each adsorbate. NH_3 adsorption leaves Cu in the Cu^{II} state, consistent with formal charge considerations. Separate calculations show that adsorption of four NH_3 decreases the normalized Cu charge from +2 to +1.9. This reduction may in part account for the 10 % Cu^{I} detected by XANES following NO cutoff (Figure 1). This reduction, however, is insufficient to account for the 30 % Cu^{I} detected during standard SCR. Figure 2 A further shows that NO neither binds to nor reduces a 6-MR Cu^{II} under standard SCR conditions.

These DFT results are consistent with the experimental observation that no individual reactant reduces Cu^{II} to Cu^{I}. The NH_3 adsorption calculations are unchanged by co-adsorption of molecular NO or O_2 at the 6-MR Cu^{II} site. As we explored NH_3 adsorption, however, we discovered a dissociation that produces Cu-bound NH_2 and a new Brønsted acidic proton, as illustrated in the bottom reaction path in Figure 3. This HSE06-computed energy is +119 kJ mol^{-1} and thus this reaction is unlikely to occur at temperatures as low as 473 K. However, the computed Cu oxidation state is +1.55, intermediate between Cu^{I} and Cu^{II} and suggesting that NH_3 dissocia-

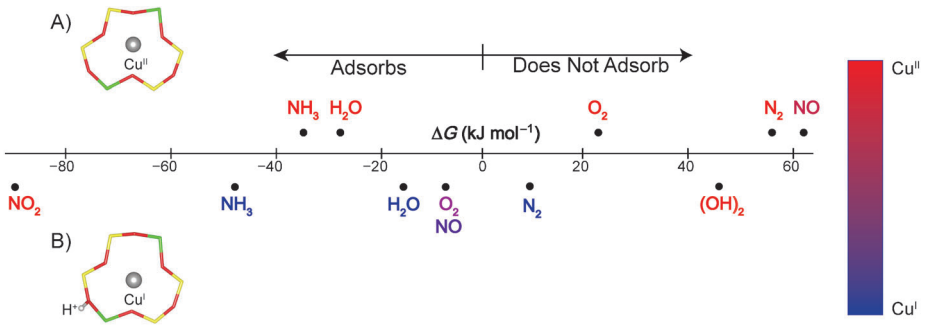

Figure 2. DFT-computed adsorption free energy (horizontal scale) and Cu oxidation state (color scale) on A) 6-MR Cu^{II} and B) 6-MR Cu^{I} plus Brønsted site. NO_2 and $(OH)_2$ energies referenced to $^1/_2 O_2$ and NO/H_2O.

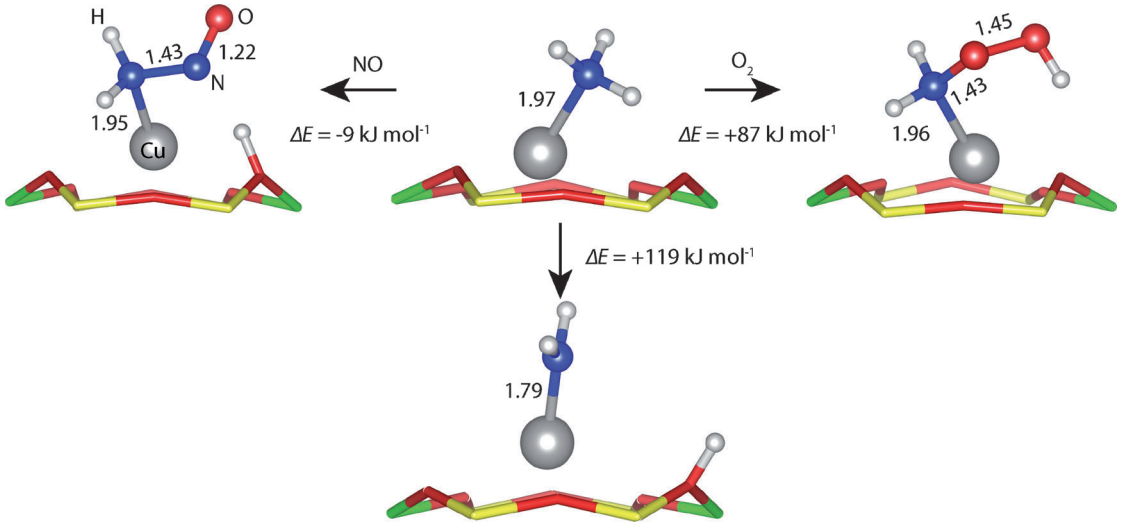

Figure 3. HSE06-computed structures and energies of NH_3 dissociation (center), NO-assisted dissociation (left), O_2-assisted dissociation (right), and products.

tion is a possible route to Cu reduction. We next explored NO co-adsorbed with this dissociated NH_3 and found that NO binds at the NH_2 nitrogen to form an H_2NNO intermediate (left path, Figure 3) reminiscent of that created from the gas-phase reaction of H_2N and NO radicals. The computed N–N bond energy is 128 kJ mol^{-1}, less than the corresponding gas-phase H_2N-NO bond energy of 226 kJ mol^{-1} [21] and reflecting the geometric distortions associated with adsorbing the intermediate on Cu. Figure 5 shows that NH_3 adsorption followed by NO-assisted dissociation has a computed free energy change close to zero and decreases the normalized Cu charge from +2 to +1. The H_2NNO intermediate has the proper stoichiometry to decompose to N_2 and H_2O; in the gas phase it does so by successive proton transfers.[21] As shown in Figure 5, the decomposition free energy to N_2, H_2O, Cu^I, and a new Brønsted acid site is −288 kJ mol^{-1}.

We contrasted this NO/NH_3 co-reaction with O_2-assisted NH_3 activation. Starting from dissociated NH_3 and O_2, the Brønsted proton relaxes away from the framework to form an H_2NOOH adduct (Figure 3). The net reaction energy is +87 kJ mol^{-1}, the Bader-derived Cu oxidation state remains +2, and no new Brønsted site is created. This selective NH_3 activation by NO over O_2 on the 6-MR Cu^{II} site is likely a key to the overall selectivity of the catalysis.

We used this observation of Cu^{II} reduction by NO and NH_3 to test the DFT-predicted creation of one Brønsted acid site with each reduction of an isolated Cu^{II} to a Cu^I ion. Experimental details on Cu^I generation and titration of excess Brønsted sites are provided in Section S8. As shown in Figure 4, the number of excess H^+ sites titrated on reduced Cu^I-SSZ-13 samples was equal, within experimental error, to the total number of Cu^I sites generated, consistent with the stoichiometric reduction of isolated Cu^{II} ions to Cu^I/H^+ site pairs. The direct experimental observation of in situ H^+ sites formed during Cu^{II} reduction to Cu^I during standard SCR suggests that NH_4^+ intermediates bound at H^+ sites proximal to Cu^I ions, but not at distant H^+ sites that remain after Cu exchange,[9] participate in the standard SCR catalytic cycle.

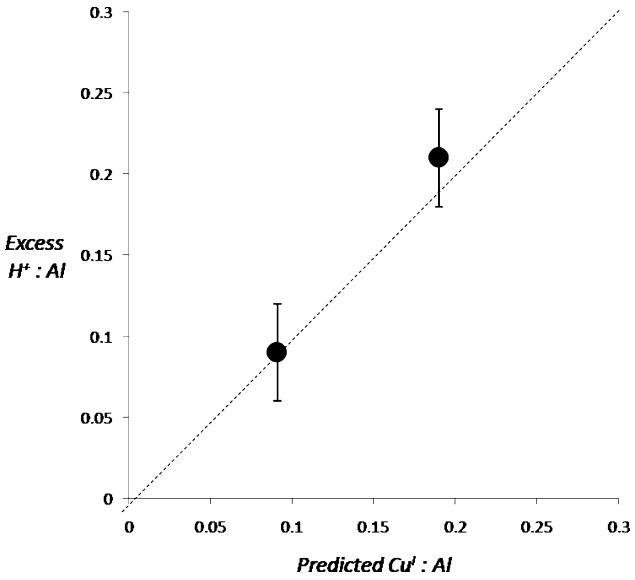

Figure 4. NH_3 titration of excess H^+ sites formed upon reduction of Cu-SSZ-13 samples after treatment in flowing NO + NH_3 (473 K).

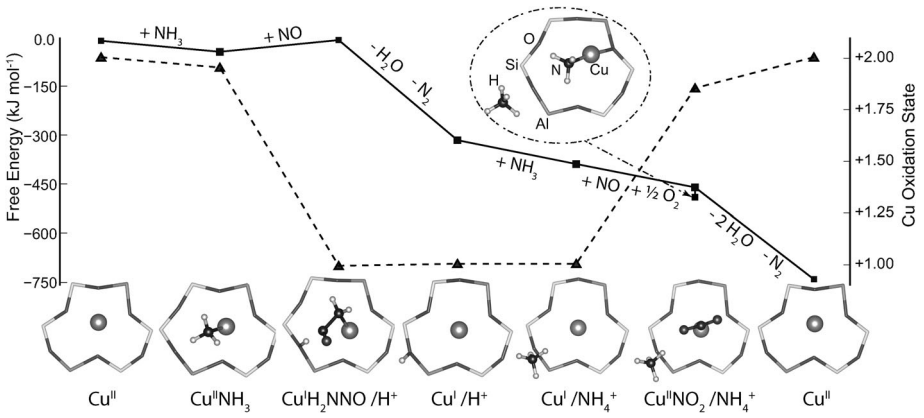

Figure 5. HSE06-computed reaction free energies (squares) and Cu oxidation state (triangles) along the standard SCR pathway. Free energies at 473 K, 1 atm, 300 ppm NH_3 and NO, 10% O_2, 5% H_2O, and 60 ppm N_2 (20% conversion). The circled species is NH_3 co-adsorbed on proximal Cu^I and Brønsted sites.

O_2 cutoff experiments provide insight into the re-oxidation of Cu^I. Steady-state NO conversion over Cu-SSZ-13 under SCR conditions decreased to zero after O_2 cut-off. As shown in Figure 1, the Cu^I content increases to 75–95% in a gas mixture containing only the NH_3 and NO reactants. Corresponding XANES spectra are in Section S6.3. O_2 is thus necessary for catalytic SCR turnovers, and specifically required for the re-oxidation of Cu^I to Cu^{II}.

To model the oxidation half-cycle, we began with the same Cu 6-MR model, now starting from the reduced Cu^I/H^+ site. We computed 473 K adsorption free energies of the same reactants following the approach above; results are shown in Figure 2B and Section S13. In general, adsorption is stronger on the Cu^I than on the Cu^{II} site. NH_3 binds most strongly to the Cu^I site, while H_2O, O_2, and NO bind weakly and N_2 does not adsorb. Of these only O_2 oxidizes the Cu to any extent, but its binding is too weak to account for the observed Cu oxidation.[4a] NH_3 binds even more strongly to the proximal Brønsted acid site to form the NH_4^+ intermediate shown in Figure 5. Computed adsorption free energies on the Brønsted and Cu^I sites are −78 and −45 kJ mol^{-1}, respectively.

As with Cu^{II} reduction to Cu^I, individual reactants cannot account for the observed Cu^I re-oxidation, so we sought oxidizing species generated from O_2 and another reactant. DFT calculations show that a dihydroxy adduct formed from H_2O and $^1/_2\,O_2$ oxidizes Cu^I to Cu^{II} (Figure 2, $(OH)_2$, and Section S10). Similarly, NO_2 formed from NO and $^1/_2\,O_2$ both binds strongly and oxidizes Cu^I to Cu^{II} (Figure 2) to form an adsorbed nitrite.[22] The exact mechanism of this NO oxida-

tion remains to be determined but could occur via a route similar to the gas phase, in which two NO and O_2 combine at the site to produce adsorbed nitrite and a second NO_2 that is consumed in a subsequent pass through the catalytic cycle. Ruggeri et al.[23] demonstrated through chemical trapping that NO_2 forms on isolated Fe sites in exchanged ZSM-5, and a similar mechanism is plausible on Cu sites in SSZ-13. We cannot categorically rule out other oxidizing intermediates, however.

Co-adsorption of NO_2 on the Cu site and NH_3 on the proximal Brønsted site is both low in energy (Figure 5) and produces an $(NH_4^+)(NO_2^-)$ complex of the correct stoichiometry to decompose into two H_2O and one N_2 molecules, consuming the Brønsted site and leaving behind the original 6-MR Cu^{II} site. Similar mechanisms involving a proximal site generated in situ have been proposed for selective reaction on supported Rh-Re bimetallic and supported vanadia catalysts.[24] Other NH_4^+ species exist in Cu-SSZ-13, bound at residual H^+ sites that remain after Cu ion-exchange,[9] but only NH_4^+ sites proximal to the Cu–nitrite species participate directly in the catalytic cycle at the SCR conditions considered here.

Scheme 1 summarizes the SCR redox mechanism inferred from the experimental and DFT findings. A 6-MR Cu^{II} site is in quasi-equilibrium with bound H_2O and with bound NH_3. NO-assisted dissociation of NH_3 occurs selectively in the presence of excess O_2 and reduces Cu^{II} to Cu^{I} while producing

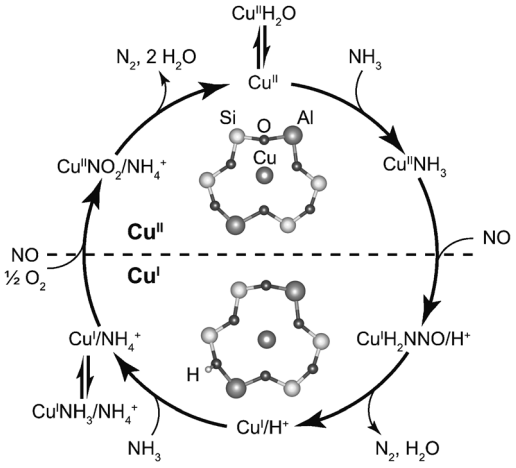

Scheme 1. Proposed SCR cycle over Cu-SSZ-13 at 473 K. The dotted line separates oxidized Cu (top) from reduced (bottom) halves of the redox cycle.

an H_2NNO intermediate and proximal Brønsted acid site. The H_2NNO intermediate decomposes to H_2O and N_2. The in situ Brønsted acid site proximal to the Cu site adsorbs NH_3 to form an NH_4^+ ion. At this point the active site consists of a Cu^{I} and a NH_4^+ ion balancing the two framework Al anions. NH_3 binds strongly to the Cu^{I} site, consistent with the NH_3 inhibition observed at super-stoichiometric NH_3 conditions.[5a] NO_2 formed directly on this Cu site or indirectly on other sites competes with adsorbed NH_3 and oxidizes the Cu site. The adjacent NO_2^- and NH_4^+ ions decompose to generate two H_2O molecules and N_2. In the overall SCR catalytic cycle, the desired product (N_2) is thus formed in both the reduction and oxidation half-cycles, which is an unexpected and unusual finding among known redox catalytic cycles.

Several of the steps in Scheme 1 are non-elementary and require work to be fully characterized. Kinetic models based on DFT-derived equilibrium constant and an assumed rate determining oxidation or reduction half-cycle invariably predict either 100% Cu^{I} or Cu^{II} sites at steady state. We surmise that both half-reactions are kinetically relevant at standard SCR conditions on the isolated Cu ions of SSZ-13. Consistent with the kinetic relevance of both half-reactions, standard SCR rates do not correlate with either the number of Cu^{I} or Cu^{II} sites observed in operando XANES.[12] The rates of these and potential competing steps, and even the nature of the active site, may also change with temperature and reaction conditions.

These experimental and computational findings highlight the redox and bifunctional nature of the Cu-SSZ-13 active site during standard NH_3-SCR. Catalysis is associated with a closed redox cycle between Cu^{II} and Cu^{I}/H^+ forms of a 6-MR site containing two framework Al atoms. Observation of both forms of the site under differential steady-state conditions indicates that both reduction and re-oxidation are relevant to observed SCR kinetics. Isolated Cu^{II} exchange sites on SAPO-34 and other zeolites likely catalyze SCR by a similar mechanism.

Received: July 9, 2014
Published online: September 12, 2014

Keywords: density functional calculations · heterogeneous catalysis · nitrogen oxides · operando spectroscopy · zeolites

[1] S. Brandenberger, O. Kroecher, A. Tissler, R. Althoff, *Catal. Rev. Sci. Eng.* **2008**, *50*, 492 – 531.
[2] J. H. Kwak, D. Tran, S. D. Burton, J. Szanyi, J. H. Lee, C. H. F. Peden, *J. Catal.* **2012**, *287*, 203 – 209.
[3] U. Deka, A. Juhin, E. A. Eilertsen, H. Emerich, M. A. Green, S. T. Korhonen, B. M. Weckhuysen, A. M. Beale, *J. Phys. Chem. C* **2012**, *116*, 4809 – 4818.
[4] a) J.-S. McEwen, T. Anggara, W. F. Schneider, V. F. Kispersky, J. T. Miller, W. N. Delgass, F. H. Ribeiro, *Catal. Today* **2012**, *184*, 129 – 144; b) F. Giordanino, E. Borfecchia, K. A. Lomachenko, A. Lazzarini, G. Agostini, E. Gallo, A. V. Soldatov, P. Beato, S. Bordiga, C. Lamberti, *J. Phys. Chem. Lett.* **2014**, *5*, 1552 – 1559.
[5] a) S. A. Bates, A. A. Verma, C. Paolucci, A. A. Parekh, T. Anggara, A. Yezerets, W. F. Schneider, J. T. Miller, W. N. Delgass, F. H. Ribeiro, *J. Catal.* **2014**, *312*, 87 – 97; b) F. Göltl, R. E. Bulo, J. Hafner, P. Sautet, *J. Phys. Chem. Lett.* **2013**, *4*, 2244 – 2249.
[6] J. H. Kwak, H. Y. Zhu, J. H. Lee, C. H. F. Peden, J. Szanyi, *Chem. Commun.* **2012**, *48*, 4758.
[7] F. Gao, E. D. Walter, E. M. Karp, J. Luo, R. G. Tonkyn, J. H. Kwak, J. Szanyi, C. H. F. Peden, *J. Catal.* **2013**, *300*, 20 – 29.
[8] A. A. Verma, S. A. Bates, T. Anggara, C. Paolucci, A. A. Parekh, K. Kamasamudram, A. Yezerets, J. T. Miller, W. N. Delgass, W. F. Schneider, F. H. Ribeiro, *J. Catal.* **2014**, *312*, 179 – 190.
[9] S. A. Bates, W. N. Delgass, F. H. Ribeiro, J. T. Miller, R. Gounder, *J. Catal.* **2014**, *312*, 26 – 36.

[10] a) J. H. Kwak, D. Tran, J. Szanyi, C. H. F. Peden, J. H. Lee, *Catal. Lett.* **2012**, *142*, 295 – 301; b) S. T. Korhonen, D. W. Fickel, R. F. Lobo, B. M. Weckhuysen, A. M. Beale, *Chem. Commun.* **2011**, *47*, 800 – 802; c) U. Deka, I. Lezcano-Gonzalez, B. M. Weckhuysen, A. M. Beale, *ACS Catal.* **2013**, *3*, 413 – 427.
[11] D. E. Doronkin, M. Casapu, T. Günter, O. Müller, R. Frahm, J.-D. Grunwaldt, *J. Phys. Chem. C* **2014**, *118*, 10204 – 10212.
[12] V. F. Kispersky, A. J. Kropf, F. H. Ribeiro, J. T. Miller, *Phys. Chem. Chem. Phys.* **2012**, *14*, 2229 – 2238.
[13] J. H. Kwak, J. H. Lee, S. D. Burton, A. S. Lipton, C. H. F. Peden, J. Szanyi, *Angew. Chem. Int. Ed.* **2013**, *52*, 9985 – 9989; *Angew. Chem.* **2013**, *125*, 10169 – 10173.
[14] F. Gao, J. H. Kwak, J. Szanyi, C. H. F. Peden, *Top. Catal.* **2013**, *56*, 1441 – 1459.
[15] D. Klukowski, P. Balle, B. Geiger, S. Wagloehner, S. Kureti, B. Kimmerle, A. Baiker, J. D. Grunwaldt, *Appl. Catal. B* **2009**, *93*, 185 – 193.
[16] a) R. M. Koros, E. J. Nowak, *Chem. Eng. Sci.* **1967**, *22*, 470; b) R. J. Madon, M. Boudart, *Ind. Eng. Chem. Fund.* **1982**, *21*, 438 – 447.
[17] a) R. B. Getman, Y. Xu, W. F. Schneider, *J. Phys. Chem. C* **2008**, *112*, 9559 – 9572; b) F. Göltl, J. Hafner, *J. Chem. Phys.* **2012**, *136*, 064503 – 064531.
[18] A. L. Myers, *Colloids Surf. A* **2004**, *241*, 9 – 14.
[19] B. Hunger, M. Heuchel, L. A. Clark, R. Q. Snurr, *J. Phys. Chem. B* **2002**, *106*, 3882 – 3889.
[20] L. Garden, G. Kington, *Trans. Faraday Soc.* **1956**, *52*, 1397 – 1408.
[21] D. Sun, W. F. Schneider, J. B. Adams, D. Sengupta, *J. Phys. Chem. A* **2004**, *108*, 9365 – 9374.
[22] W. F. Schneider, K. C. Hass, R. Ramprasad, J. B. Adams, *J. Phys. Chem. B* **1998**, *102*, 3692 – 3705.
[23] M. P. Ruggeri, T. Selleri, M. Colombo, I. Nova, E. Tronconi, *J. Catal.* **2014**, *311*, 266 – 270.
[24] a) M. Chia, Y. J. Pagan-Torres, D. Hibbitts, Q. Tan, H. N. Pham, A. K. Datye, M. Neurock, R. J. Davis, J. A. Dumesic, *J. Am. Chem. Soc.* **2011**, *133*, 12675 – 12689; b) N. Y. Topsoe, J. A. Dumesic, H. Topsoe, *J. Catal.* **1995**, *151*, 241 – 252.

